Time-Resolved Fourier Transform Infrared Emission Spectroscopy of NH Radical in the $X^3\Sigma^-$ Ground State

Adam Pastorek , Victoria H.J. Clark , Sergei N. Yurchenko , Svatopluk Civiš

PII: S0022-4073(22)00267-9
DOI: https://doi.org/10.1016/j.jqsrt.2022.108332
Reference: JQSRT 108332

To appear in: *Journal of Quantitative Spectroscopy & Radiative Transfer*

Received date: 16 March 2022
Revised date: 20 July 2022
Accepted date: 24 July 2022

Please cite this article as: Adam Pastorek , Victoria H.J. Clark , Sergei N. Yurchenko , Svatopluk Civiš , Time-Resolved Fourier Transform Infrared Emission Spectroscopy of NH Radical in the $X^3\Sigma^-$ Ground State, *Journal of Quantitative Spectroscopy & Radiative Transfer* (2022), doi: https://doi.org/10.1016/j.jqsrt.2022.108332

Time-Resolved Fourier Transform Infrared Emission Spectroscopy of NH Radical in the $X^3\Sigma^-$ Ground State

Adam Pastorek[1,2], Victoria H.J. Clark[3], Sergei N. Yurchenko[3], Svatopluk Civiš[1,*]

1 – J. Heyrovský Institute of Physical Chemistry, Czech Academy of Sciences, Dolejškova 2155/3, 18200, Prague 8, Czech Republic
2 – Faculty of Nuclear Sciences and Physical Engineering, Czech Technical University in Prague, Břehová 78/7, 11519, Prague 1, Czech Republic
3 – Faculty of Mathematical and Physical Sciences, University College London, Gower Street, London WC1E 6BT, United Kingdom

** Corresponding author*

Highlights

- T-R FTIR spectroscopy of NH radical
- Generation of species in glow discharge of N_2+H_2 and N_2+NH_3+Ar mixtures
- Analysis of decomposition products together with time profiles
- Pure rotation transitions first observed in the lab by use of cold source
- Non-LTE modelling of obtained spectra

The NH radical is an extremely important specie in nitrogen chemical reaction networks, in the interstellar medium and atmospheric chemistry. Time resolved Fourier transform spectroscopy technique in the frequency range 10-13 μm has been applied for the measurement of a pure rotational spectrum of the NH free radical (NH) in the ground $X^3\Sigma^-$ electronic state. Twelve high *N* (26-29) triplet-resolved pure rotation lines of NH were experimentally observed in the laboratory and compared with satellite ACE (Atmospheric Chemistry Experiment) solar data. In addition, discharge-generated vibration-rotation NH radical bands in the spectral range 1923-3571 cm^{-1} have been measured with a microsecond time resolution and spectral resolution of 0.02 cm^{-1}. The spectra of the NH radical have been studied in two experimental arrangements. Firstly, in a pulsed positive column discharge of pure hydrogen-nitrogen mixture and secondly, in a discharge of nitrogen-ammonia mixture in

the presence of argon buffer gas. Both production methods are described and compared. The population analysis of the experimental spectra was performed via modelling using the accurate MoLLIST line lists for NH. It was shown that laboratory data can be well reproduced by use of a mixture of the local-thermal-equilibrium (LTE) and non-LTE models corresponding to high temperatures (up to 8000 K and up to 6000 K rotational).

Keywords

NH radical; NH - high-resolution vibration-rotation molecular spectra; NH - rotational spectra; Spectral (non-LTE) modelling; Atmospheric molecular species; Molecular astrophysics

Introduction

There have been many infrared and far infrared studies of NH aimed at extracting precise molecular and hyperfine constants in the ground electronic $X^3\Sigma^-$ state. The first vibration-rotational infrared spectrum of imine radical (1-0 band) was collected by Bernath and Amano in 1982.[1] In 1986 Boudjaadar *et al.*[2] observed the $\Delta v = 1$ sequence of the NH spectrum up to 5-4 band. Line strengths of rovibrational lines and rotational transitions within the ground electronic state are given by J. Brooke *et al.*[3] Doppler-limited rotational spectrum of the NH radical in its ground electronic $X^3\Sigma^-$ and its vibrationally excited states have been measured using the frequency stabilized Cologne side band spectrometer in the frequency range near 2 THz.[4]

From the chemical point of view, focusing mainly on the synthesis of the imine radical itself, K. Stewart[5] demonstrated the main possibilities of NH radical synthesis in the lab for scientific purposes. Especially, the production of NH by azoimide decay process by active nitrogen was highlighted. A recent Helden *et al.* study about the NH reaction describes the mechanism of NH formation inside of the hydrogen-nitrogen plasma mixture.[6]

NH is a free radical important in atmospheric chemistry. This radical was first detected in 1893 by Eder[7] by his photographic detection near 336 nm and has been the subject of many subsequent investigations. In 1919, the imine radical was found in solar spectra by Fowler *et al.*[8] and in 1930s by Funke[9] who has assigned the main emission branches of the electronic 0-0 and 1-1 bands of $A^3\Pi$-$X^3\Sigma^-$ system around the 29000 cm^{-1} spectral wavenumber. The analysis was greatly improved by the observation of the bands in absorption by Dixon[10] from an electronic spectrum that was for a long time the main source of information on this radical. A more complete review related to electronic spectroscopy can be found in Ram *et al.* (1999)[11] and others (see below).

Since the discovery of NH in solar spectra, this radical became quickly important among astrophysicists and new extensive studies focusing on pure fundamental spectroscopy of NH produced by relatively cool laboratory sources appeared. Notable examples of NH synthesis are flash photolysis of isocyanic acid,[10] photolysis of ammonia mixed with an inert gas,[12] UV photolysis of ammonia and consequent resonant fluorescence of NH,[13] electric discharge of hydrogen and nitrogen in a hollow cathode[14] or modern two-photon capture on ammonia in a flow reactor by tuneable laser[15].

NH radical is for example used in calculating nitrogen abundance in stars and in interstellar space. NH was detected in comets, e.g. comet Cunningham,[16] together with other radicals such as CN, OH and CH. Cometary NH can also be used in calculations of photodissociation lifetimes. The photodissociation lifetimes of the NH radical through absorption of solar radiation into the $A^3\Pi_i$ state have been calculated as a function of the heliocentric velocity of the comet, and the velocity distributions of the product atoms were determined by P. Singh.[17] NH can also be found in cool stars, for example HD 122563,[18] a metal-poor star. Rovibronic transitions of NH have been observed on Betelgeuse,[19] the second brightest star in the Orion constellation. V. Smith *et al.* found NH in 12 red giants[20] and used to calculate the abundance of carbon, nitrogen, oxygen and other elements. Similar publication was the work of Aoki *et al.*,[21] who studied the high resolution spectra of K and M class giants and correctly highlighted the advantage of nitrogen abundance calculation by use of NH radical spectra in comparison with CN.

The first proof of interstellar existence of NH was the publication by D. Meyer[22] from 1991, which demonstrated presence of this radical in a diffuse cloud around ζ Persei and HD 27778. The spectra of NH radical were recorded in the UV region and were assigned to the well-known $A^3\Pi - X^3\Sigma$ band. Later, in 1997, NH was also found in a diffuse cloud close to ζ Ophiuchi, a bright star approx. 366 light-years from Earth.[23] Data acquired during this observation effectively disproved the theory of the so-called hot formation of NH, when NH is formed by synthesis of nitrogen and hydrogen with a subsequent formation of atomic hydrogen, and supported the hypothesis of formation of NH on dust grain surface in diffuse molecular clouds as a main source of interstellar NH. This theory was also supported by Weselak *et al.* in 2009.[24]

A possible complex origin of nitrogen in metal-poor stars was a subject to study for Spite *et al.* in 2005.[25] The main goal of this publication was to describe possible reaction pathways of the origin of light elements in the early stages of the existence of our Galaxy. The authors computed the abundance ratios and generated mixing models used for the estimation of the mixing of various layers of stars. By comparing the data from 35 different stars, the work suggested the abundance of gases on stellar surfaces which did not undergo any mixing.

As for any astronomically important species, NH radical also found its place in many purely theoretical publications. One of the first *ab initio* calculations, published in 1970,[26] focused on determination of the bond length of NH. G. Das *et al.*[27] published five rovibrational

spectroscopic constants of NH via a Dunham fit. Ram *et al.*[28] obtained spectroscopic constants for $X^3\Sigma$ and $A^3\Pi$ states of NH via analysis of the existing experimental data. The constants are being improved until today.[3,29,30]

In past 20 years, a new application of the NH radical emerged, when it was found to be a relevant medium for the research of magnetic molecular traps.[31] These traps are used for the research of physical behaviour of extremely cold and dense matter. A metastable energy state of NH, $a^1\Delta$, is used in such experiments due to its desirable properties. The deceleration of NH is realized e.g. by Stark[32] or Zeeman decelerators.[33] These experiments, ideally leading to completely slowed NH radicals of high local density, have potential application in quantum computers.

In this paper, both the rotational spectrum of the NH radical in the ground $X^3\Sigma^-$ electronic state (the frequency region of 700-1000 cm^{-1}) and compared with ATMOS and ACE Solar data. The infrared rovibrational spectrum of NH in its ground $X^3\Sigma^-$ electronic state (1923 - 3571 cm^{-1} spectral range) have been observed and studied using the time resolved Fourier transform spectroscopy technique.

Experimental apparatus

Instrumentation of spectral measurements

A specially designed discharge tube was used in all measurements and experiments. Its scheme is depicted in Figure 1 below. Infrared emission was observed from a pulsed discharge of FT time-resolved measurements. The parent compound hydrogen or ammonia was entrained in an inert carrier gas (N_2, Ar) and transferred into the 20 cm long positive column discharge tube with an inner diameter of 12 mm. The pulsed discharge was induced by a high voltage transistor switch HTS 81 (Behlke electronic GmbH, Frankfurt, Germany) between a stainless-steel anode and a grounded cathode. The plasma produced from the reaction mixture was cooled by flowing water in the outer jacket of the cell. The voltage across the both electrodes varied from 1 to 1.4 kV and the electric current was 150-300 mA. The scanner velocity of the FT spectrometer was set to produce a 10 kHz He–Ne laser fringe frequency which was used to trigger the pulsed discharge. The emission radiation from the discharge cell was focused into the aperture of the spectrometer by a lens. The aperture diameter was set to 2 mm.

The spectra were obtained by use of the Bruker IFS 120 HR spectrometer with KBr optics, HgCdTe detector and a KBr beam splitter and separately CaF_2 optics, InSb detector and CaF_2 beam splitter. The broad spectral region was cut by optical interference filters with transparency either in the range of 700-900 cm^{-1} or 1923 - 3571 cm^{-1}. The unapodized spectral resolution was 0.02 cm^{-1}.

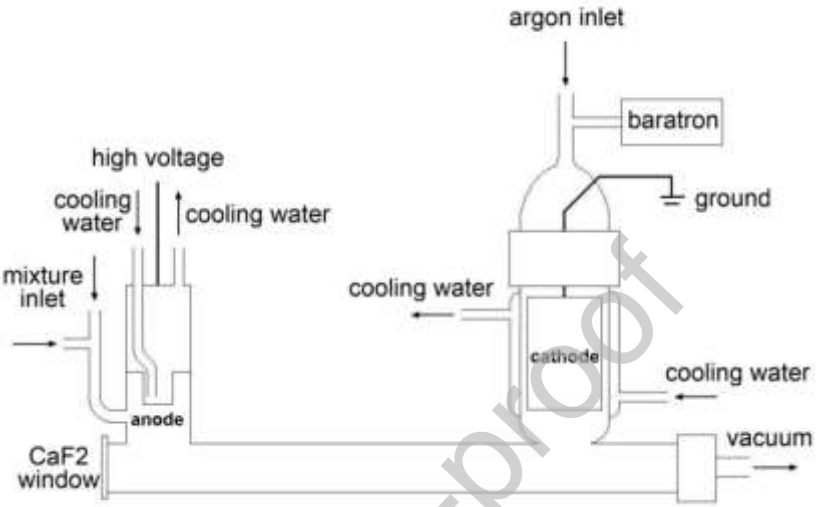

Figure 1: The discharge cell

The discharge was realized either with a mixture of hydrogen and nitrogen (pressure ratio 1:1, total pressure of 3 Torr), or with a mixture of nitrogen and ammonia in argon buffer gas. In the latter case, the pressure was 0.5 Torr of argon, 0.8 Torr of nitrogen and 0.1 Torr of ammonia.

Time -resolved spectroscopy

Time-resolved Fourier transform spectroscopy (TR-FTS) is a wide-spectrum technique used for studying the dynamics of chemical reactions, or the dynamic properties of molecules, radicals and ions in gas, liquid and solid states. The main advantage of TR-FTS lies in obtaining spectra in wide wavenumber intervals and in a possibility to study the dynamical change of the spectral characteristics during the evolution of the discharge plasma, where each ion, atom or molecule has its own lifetime. Therefore, the knowledge of the lifetime in the set of time-shifted spectra can help in the spectral analysis of the data. The fundamental principles of our time resolution system are depicted in Figure 2.

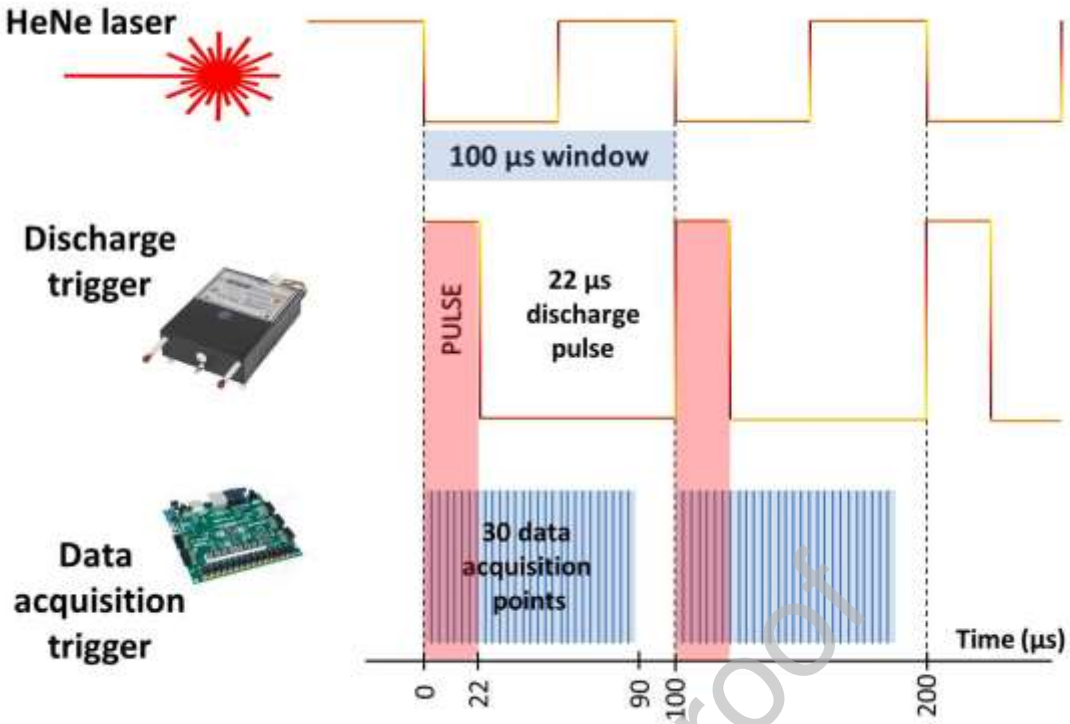

Figure 2: Time-resolved data acquisition setup

Time resolved interferograms are obtained by collecting data at various points between the zero-crossings of the HeNe laser pulses. Each interferogram is then transformed by FT to a spectrum. This system contains an FPGA processor. The main role of the FPGA processor in our experiment is to create a discharge or laser pulse and AD trigger signals (the signal for data collection from the detector) synchronously with the He–Ne laser fringe signals from the spectrometer (see Figure 2). The FPGA processor also controls the data transmission from the digital input board to the PC.

Between 30 and 100 scans, depending on the sample, were coadded so as to obtain a reasonable signal-to-noise ratio. The observed wavenumbers were calibrated using CO emission rotation-vibration lines. After each pulse, which generated the discharge plasma, we collected a spectrum every 2 or 3 µs for 60 or 90 µs (30 spectra after each pulse). Similar or identical experimental arrangement can be found in our previous papers, e.g. Pastorek *et al*. (2021),[34] Horká *et al*. (2004),[35] Ferus *et al*. (2011)[36] or Ferus *et al*. (2019).[37]

In this work, the spectra of the NH radical were recorded in the glow discharge of two mixtures, H_2 + N_2 (in the 2400-3600 cm^{-1} region) and NH_3 + N_2 + Ar (in two regions, 2400-3600 cm^{-1} and 700-900 cm^{-1}).

Results and discussion

Figure 3 show the overall spectra of NH radical in 2400-3600 cm^{-1} spectral range.

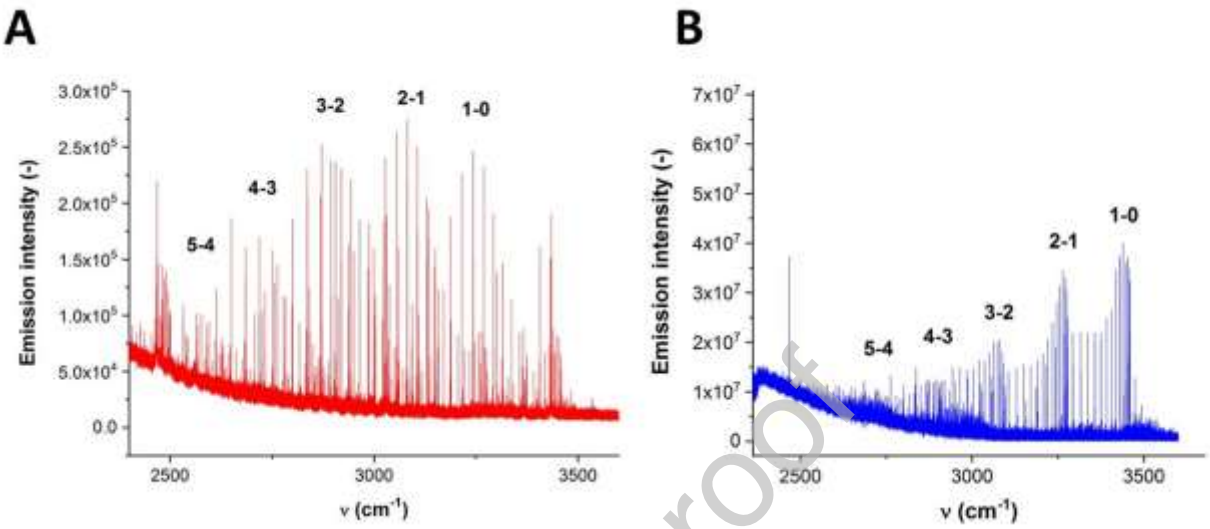

Figure 3: Panel A – averaged spectrum of H_2 + N_2 discharge
Panel B – averaged spectrum of NH_3 + N_2 + Ar discharge

In panel A of Figure 3, the spectrum of the H_2 + N_2 discharge from 6 averaged spectra from a 30-50 μs time after pulse is displayed. Each of the averaged spectra was obtained by co-adding 50 scans. The bands are marked according to vibrational transitions. The spectrum of the second mixture NH_3 + N_2 + Ar (Panel B) was produced with a better signal-to-noise ratio and a slightly different population of the rotational-vibrational bands. The Panel B spectrum was obtained by accumulation of 100 scans.

The technique presented in this work allows acquisition of the rough information about the lifetimes of selected rotational-vibrational states. The time-dependent intensity change of the individual emission line (time profile) brings the information about the relaxation processes of the individual vibration states. The relaxation process in the case of the NH radical is rather complicated, and we assume that this process starts with the fragmentation all molecules into atomic form (see Figure 4, H 4f-5g transition). This step is followed by additional interaction of hydrogen atom with carbon atom and formation the short-lived NH radical. This process takes place either in molecular nitrogen or Ar buffer gas environment. NH populated in the different excited vibration states is subsequently quenched in our relatively high-pressure

discharge conditions (units of Torr of total pressure). The decay process of the NH radical can be described and fitted by using a single exponential decay function

$$y = Ae^{-t/\tau} \quad (1)$$

where τ is the lifetime of the individual transition.

We have observed rotational-vibrational transitions in the ground electronic state $X^3\Sigma^-$ for the fundamental band and hot bands up to 5-4, see (Fig. 4). The lines of the imine radical and spectra of atoms (H I, N I) were assigned according to the literature. We have evaluated the data for fundamental and hot rotation-vibration bands for selected *J* transitions from each P and R branch and calculated their lifetimes (1). The results for several individual transitions of hot bands are summarized in Table 1.

Table 1: Classification and lifetimes of selected emission lines of the NH radical

ν (cm^{-1})	**upper–lower v**	**upper *N*, *J***	**lower *N*, *J***	**lifetime (μs)**
2778.19	4-3 (R)	5; 6	4; 5	30.8 ± 4.2
2532.12	4-3 (P)	4; 3	5; 4	25.9 ± 4.5
2919.73	3-2 (R)	4; 4	3; 3	35.9 ± 2.9
2685.03	3-2 (P)	3; 4	4; 5	37.0 ± 4.6
3081.46	2-1 (R)	4; 5	3; 4	40.6 ± 2.9
2871.51	2-1 (P)	2; 3	3; 4	45.9 ± 4.4

Several selected lines of NH from the thirty time-shifted spectra were integrated and are plotted in Figure 4 as functions of time. Time profiles of the integral intensity of the 2-1 (3081.46 cm^{-1}, J' = 5) and 1-0 (3242.96 cm^{-1}, J' = 4) as well as of the hydrogen atomic line (4f – 5g, 2467.75 cm^{-1}) are depicted in Figure 4.

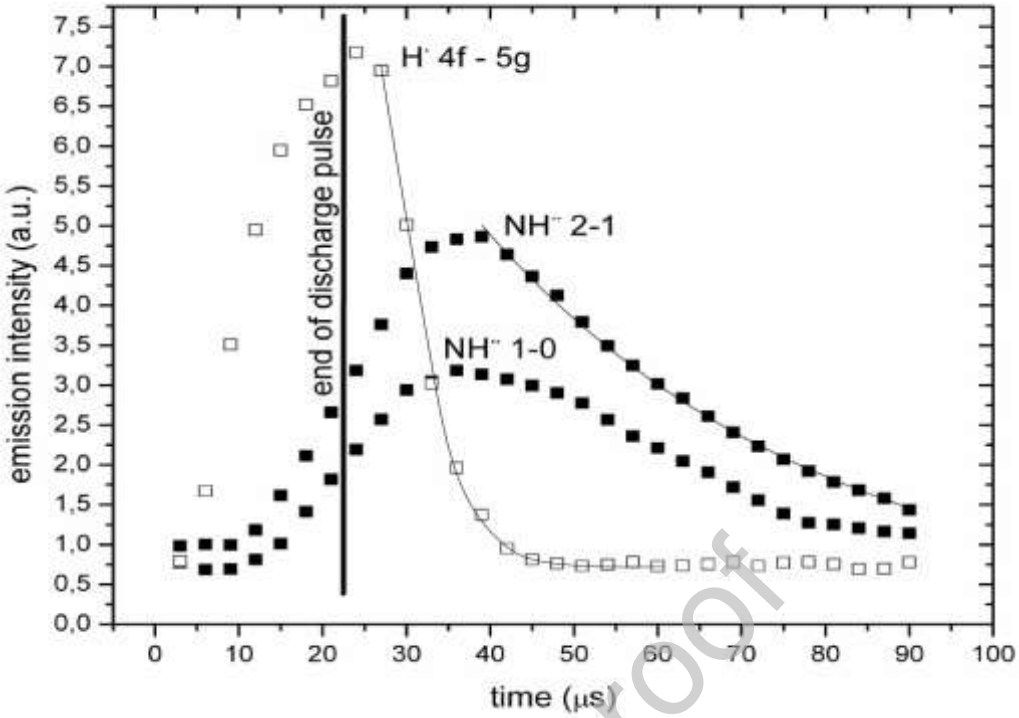

Figure 4: The time profiles of selected lines (NH (2-1) and H (4f-5g) fitted by exponential function) in the N_2 + H_2 mixture

The intensity of the NH lines is increasing during the discharge pulse (duration 22 μs) and achieves the maximum at the 39 μs. After that the line intensities of the imine radical start to diminish for all measured transitions. In comparison, the intensities of the hydrogen atomic line are increasing during the discharge and reaching the maximum exactly at the end of the discharge pulse. The decay time (about 8 μs) of the hydrogen atomic 4f-5g transition is much faster in comparison to results getting for NH transitions. The H atomic line disappears from the emission spectrum at 45 μs. The estimated values of the lifetimes (under aforementioned experimental conditions) are summarized in Table 1. The lifetime values obtained for higher vibrational levels are slightly shorter (transitions from v = 4, v = 3 and v = 2 levels correspond to 26 μs, 36 μs and 46 μs, respectively). The arising tendency of the prolongation process of lifetime values for the lower vibrational levels is in an agreement with our expectation based on our previous study of the vibrational relaxation of CN radical in the ground electronic state.[38]

We suggest that the mechanism of relaxation mechanism inside of the discharge plasma is rather complicated process, which can, for some lines, be approximately described using single exponential decay function from equation (1) (see Figure 4 - H 4g-5f and NH 2-1

transitions) but for many other transitions (for example Figure 4: NH 1-0) the decay time is difficult to reproduce with a single exponential decay function. Hence, the relaxation mechanism is more complicated and the NH radical is probably quenched via several multilevel processes.

One very important basic characteristic of the HR-FTS is the possible separation two or more different mixed spectra using the different time domain measurement.

The typical example is depicted on Fig.5. The figure shows the time profiles of selected NH and nitrogen emission lines and their time-resolved spectra at different time measurement.

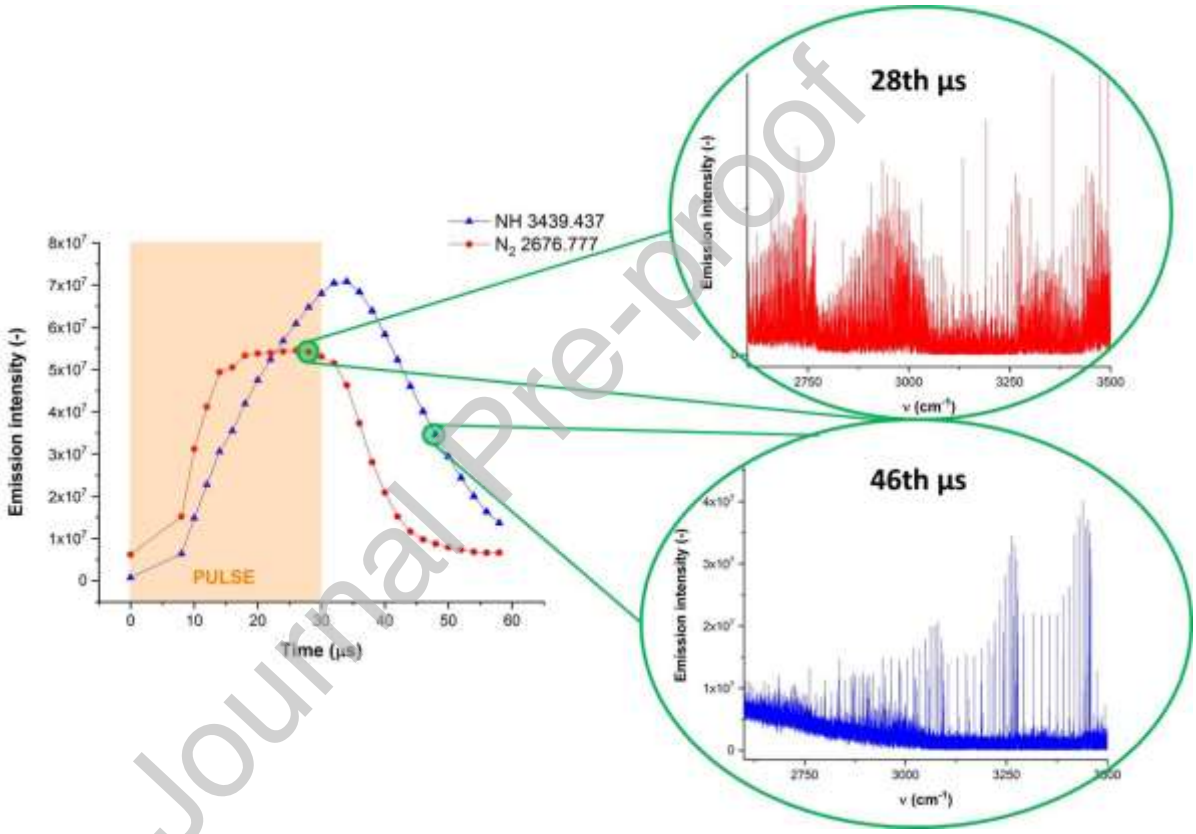

Figure 5: Time profiles of NH and N_2 and the appearance of spectra at specific times

According to the time profile curves in Figure 5, both species appear to gain energy at the end of the discharge pulse (30 μs here). At the 28th microsecond both molecular nitrogen and NH radical have a maximum intensity and the spectra of both species are blended together (Figure 5, red spectrum 28 μs). This spectrum predominantly contains molecular nitrogen lines and it is difficult to recognize any NH radical spectral lines. In contrast, at 46 μs the blue spectrum in Fig. 5 shows the NH spectrum which got rid of all N_2 molecular transition and the spectrum belongs to the NH radical only. Not having the option to measure time-resolved spectra would

result in a spectrum containing signals of all species together, where the information on the dynamics would be lost.

Pure rotational NH spectrum

Several excited pure rotational lines of NH in the v = 0 vibrational state were measured in the discharge mixture of NH_3 +N_2 + Ar. According to our best knowledge, this measurement is the first laboratory experimentally observed pure rotational NH spectrum in the spectral range between 700-900 cm^{-1}.

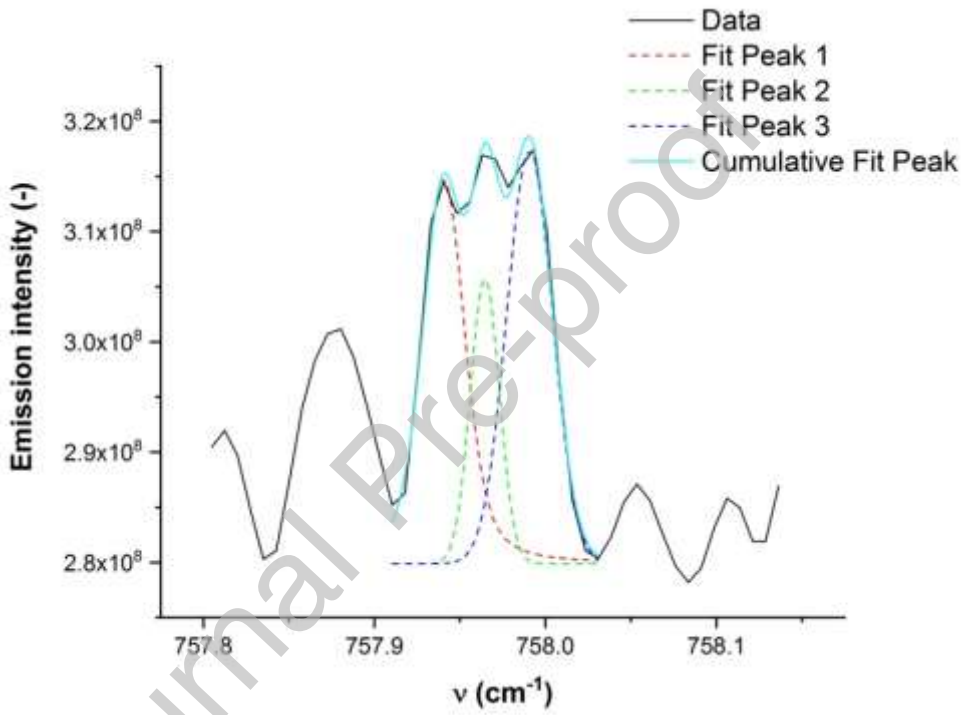

Figure 6: Deconvolution of a NH radical triplet (*N*'' = 26, v = 0)

Table 2, summarises four detected rotational transitions of NH radical in the spectral range of 750-815 cm^{-1}. All the observed emission lines are split into the triplets. From the theoretical point of view the NH radical is a linear molecular radical with an open electronic shell producing a triplet ($X^3\Sigma^-$) electronic ground state. The nonzero total electron spin angular momentum generates a fine structure of rotational *J* sublevels with *N* quantum numbers. In addition to this, nonzero nuclear spins of the nitrogen atom and the magnetic field are responsible for the magnetic (nuclear spin–rotation, dipole–dipole, and Fermi contact), and electric nuclear quadrupole interactions. Our spectral resolution, 0.02 cm^{-1} was not sufficient to resolve the hyperfine structure of the peaks. Their approximate position and shape had to

be estimated using the deconvolution method applied for each single transition represented with the unresolved triplet of lines. A simple deconvolution by use of nonlinear Voigt peak fitting in OriginPro 2018® was used.

Table 2: Overview of observed pure rotational NH lines (in cm^{-1})

N''	Assignment	Our position	Solar position*
26	^{r}R1(27)	757.940	757.936
	^{r}R2(26)	757.966	757.964
	^{r}R3(25)	757.993	757.992
27	^{r}R1(28)	776.966	776.966
	^{r}R2(27)	776.990	776.986
	^{r}R3(26)	777.014	777.009
28	^{r}R1(29)	795.104	795.099
	^{r}R2(28)	795.125	795.122
	^{r}R3(27)	795.146	795.143
29	^{r}R1(30)	812.301	812.310
	^{r}R2(29)	812.329	812.332
	^{r}R3(28)	812.355	812.360

*Solar wavenumbers in Table 2 are extracted from ATMOS (Atmospheric Trace Molecule Spectroscopy) experiment (April 29 – May 2, 1985), described and identified in publications by Farmer and Norton (1989)[39] and Geller *et al*. (1991).[40] For each *N*'' number a triplet of NH lines is described in Table 2. The assignment was adopted from Brooke et al. (2014).[3]

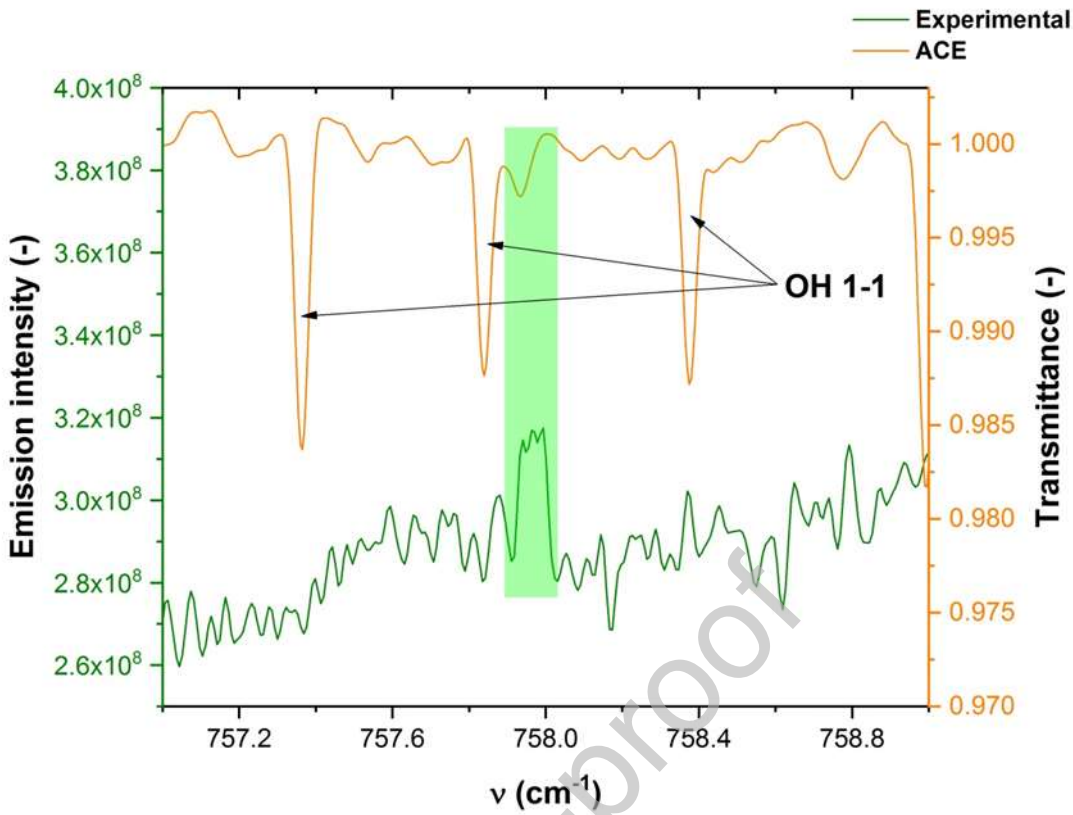

Figure 7: The comparison of ACE solar NH rotation spectrum and NH radical laboratory measurement

Figure 7 depicts the comparison of our NH radical experimental spectrum with ACE (Atmospheric Chemistry Experiment) solar spectrum. The coincidences of matching NH lines are highlighted in green colour. The line depicted in Figure 7 corresponds to *N*" = 27, v = 0 rotation transition of NH. Additional lines (Figure 7) in the solar spectrum belong to OH radical spectrum.

Rotational-vibrational spectrum of NH in the ground electronic state ($X^3\Sigma^-$)

The rotation-vibrational spectra of NH have been investigated in several laboratories. The effort of other works was already described in the introductory section.

With respect to ACE[41] (Atmospheric Chemistry Experiment) data, we compared our NH radical spectra with ACE solar spectra. The match of our and ACE NH lines can be observed in Figure 8.

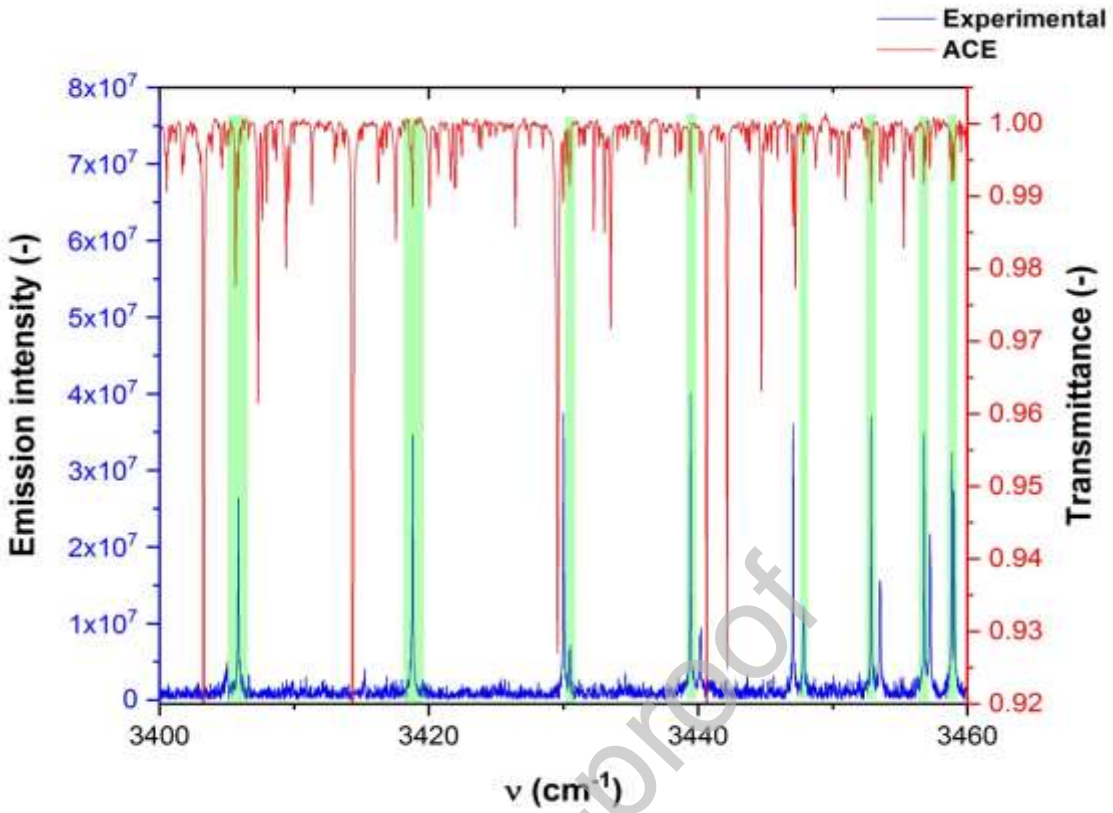

Figure 8: The comparison of ACE solar spectrum with the laboratory measured rotation-vibration NH spectrum

Figure 8 depicts the comparison of ACE solar spectrum with our NH radical rotation-vibrational NH spectrum in the spectral range 3400-3450 cm^{-1}. The coincidence with solar spectrum is highlighted in green shading. The comparison of both spectra clearly shows the different Boltzmann population of ro-vibrational transitions.

LTE vs non-LTE modelling of the spectrum of NH

In order to model the emission spectrum of NH (Figure 3), we used the line MoLLIST line list[3,29,30,42] from the ExoMol database ExoMol[43] in conjunction with the program ExoCross.[44]

We start by estimating the plasma temperatures. For the N_2 + NH_3 + Ar mixture, the vibrational temperature has been calculated from rotational-vibrational NH bands in the 2700-3500 cm^{-1} range. In the double harmonic approximation, vibrational temperature is given by the linear dependence (see Pastorek, A., Civiš, S., Clark (2021)):

$$\ln\left[\frac{I}{\nu^3(\mathrm{v}'+1)}\right] = KE_{\mathrm{v}'} + Q \tag{2}$$

where I stands for intensity, ν is the wavenumber of an edge of the selected band (wavenumber of the most intense line), v' is the vibrational quantum number of an upper energy state, K is the slope of the linear regression, $E_{\mathrm{v}'}$ is the energy of an upper v-state and Q is a constant. By linear regression of the dependence (2), the vibrational temperature is expressed by:

$$T_V = -\frac{hc}{kK} \tag{3}$$

where k is Boltzmann constant.

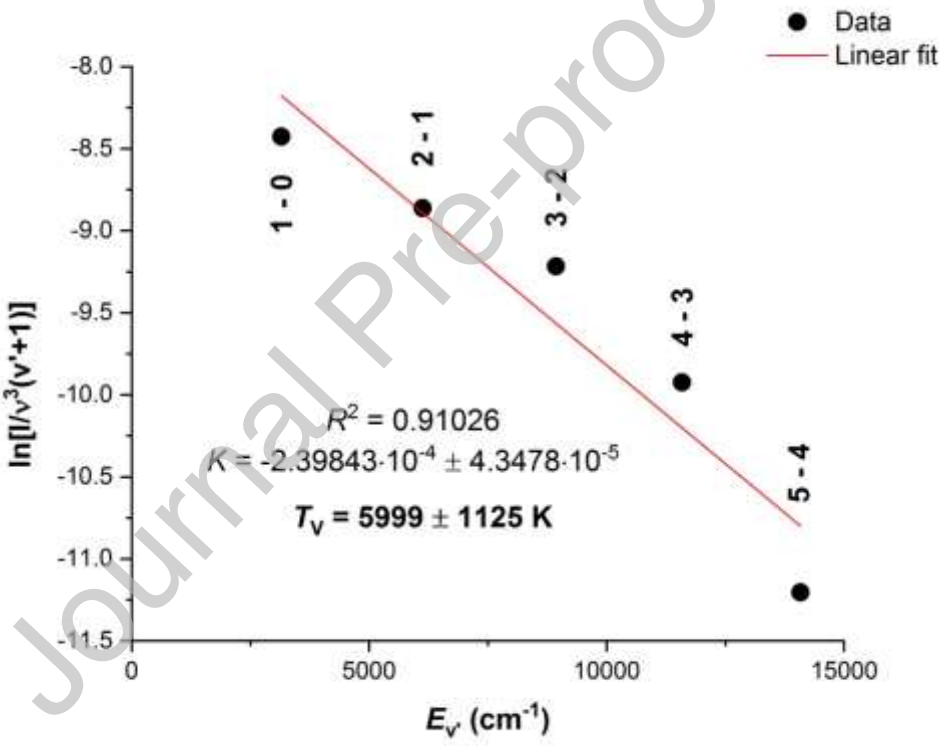

Figure 9: Estimation of vibrational temperature (v-transitions specified)

The transitions used in Figure 9 were fixed at J' = 4 and N' = 3. From the intensities of the J' = 4 and N' = 3 lines of the v = 1-0, 2-1, 3-2, 4-3 and 5-4 bands, the vibrational temperature was estimated to be T_V = 5999 ± 1125 K.

Using this value, T = 6000 K, as an equilibrium temperature, an emission spectrum of NH in the 2500–3500 cm^{-1} window was modelled. As one can see from Figure 10, where the

theoretical spectrum (bottom) is compared to the experimental spectrum (top), this temperature provides the best reproduction of the experimental spectrum. It also shows that the rotational temperature at the time of the measurement is in equilibrium with the very high vibrational temperature thus suggesting the so-called local-thermal-equilibrium (LTE) conditions.

The emission spectrum of NH from the H_2 + N_2 has a different shape and could not be modelled using the LTE conditions. The best agreement with the experiment was achieved using a non-LTE and a bi-temperature approach with different rotational and vibrational temperatures of T_R = 500 K and T_v = 8000 K, respectively. The result of the non-LTE modelling for the 2400–3600 cm^{-1} window is illustrated in Figure 11, showing good agreement with the experimental spectrum. The bi-temperature approach used is described in the following (see also Pastorek, A., Civiš, S., Clark, V. H. J., Yurchenko, S. N. & Ferus (2022)).

The non-LTE bi-temperature approach is based on the Treanor distribution[45] for energy level population, with rotational and vibrational states described by the corresponding LTE distributions. The separate temperatures for rotations and vibrations are used to calculate the respective energies, and the total energy is approximated as the sum of the rotational and vibrational energies:

$$\tilde{\mathrm{E}}_{J,\nu} = \tilde{\mathrm{E}}_{\nu}^{vib} + (\tilde{\mathrm{E}}_{J,\nu} - \tilde{\mathrm{E}}_{\nu}^{vib}) \tag{4}$$

where ν and k are the vibrational and rotational quantum numbers, respectively and $\tilde{\mathrm{E}}_{J}^{\nu,rot} = \tilde{\mathrm{E}}_{J,\nu} - \tilde{\mathrm{E}}_{\nu}^{vib}$ is the rotational energy contribution.

The non-LTE distribution of the spectrum then arises from the product of the vibrational and rotational distributions.[44,46]

$$N_{J,\nu}(T_\mathrm{v}, T_\mathrm{R}) = g_J \frac{e^{-c_2 \tilde{\mathrm{E}}_{\nu}^{vib}/T_\mathrm{v}} e^{-c_2 \tilde{\mathrm{E}}_{J}^{\nu,rot}/T_\mathrm{R}}}{Q(T)} \tag{5}$$

where $c_2 = hc/k_B$ is the second radiation constant, $\tilde{\mathrm{E}} = \mathrm{E}/hc$ is the energy term value, $g_J = g_J^{ns}\,(2J+1)$ is the state degeneracy, g_J^{ns} is the nuclear-spin statistical weight factor and T_v and T_R are the vibration and rotation temperatures, respectively. In Eq. (5), $Q(T)$ is the non-LTE partition function defined as a sum over states:

$$Q(T) = \sum g_n^{ns}(2J_n + 1)N_{J,v,k}(T_{\mathrm{v}}, T_{\mathrm{R}}) \quad (6)$$

J_n is the corresponding total angular momentum.

An emission line intensity I_{if} (in photon/s) for a transition $i \rightarrow f$ with the wavenumber $\tilde{\nu}_{if}$ is then given by

$$I(i \rightarrow f) = N_{J',v',k'}A(i \rightarrow f) \quad (7)$$

where A_{if} is the Einstein-*A* coefficient.

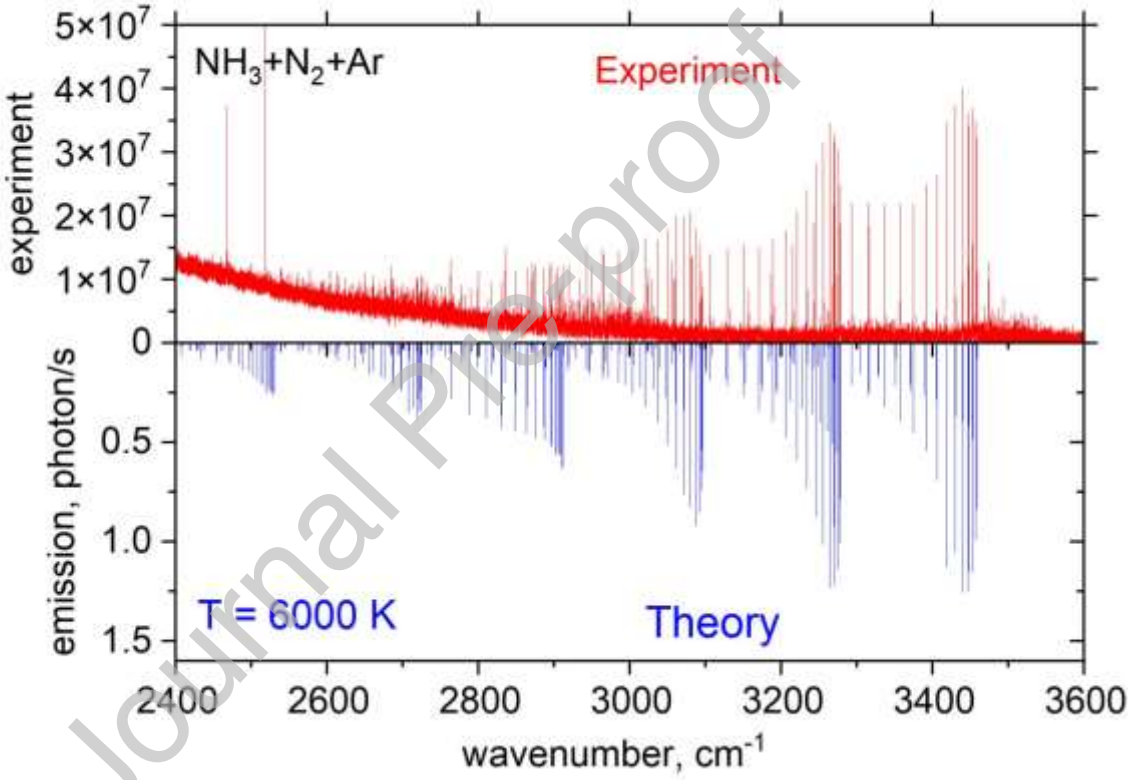

Figure 10: Experiment (red) versus theory (blue) modelling of the NH spectra between 2500-3500 cm^{-1} obtained from the NH_3 + N_2 + Ar mixture. The theoretical spectrum corresponds to T = 6000 K, Lorentzian line profile and a HWHM = 0.05 cm^{-1}. The MoLLIST[42,43] line list was used.

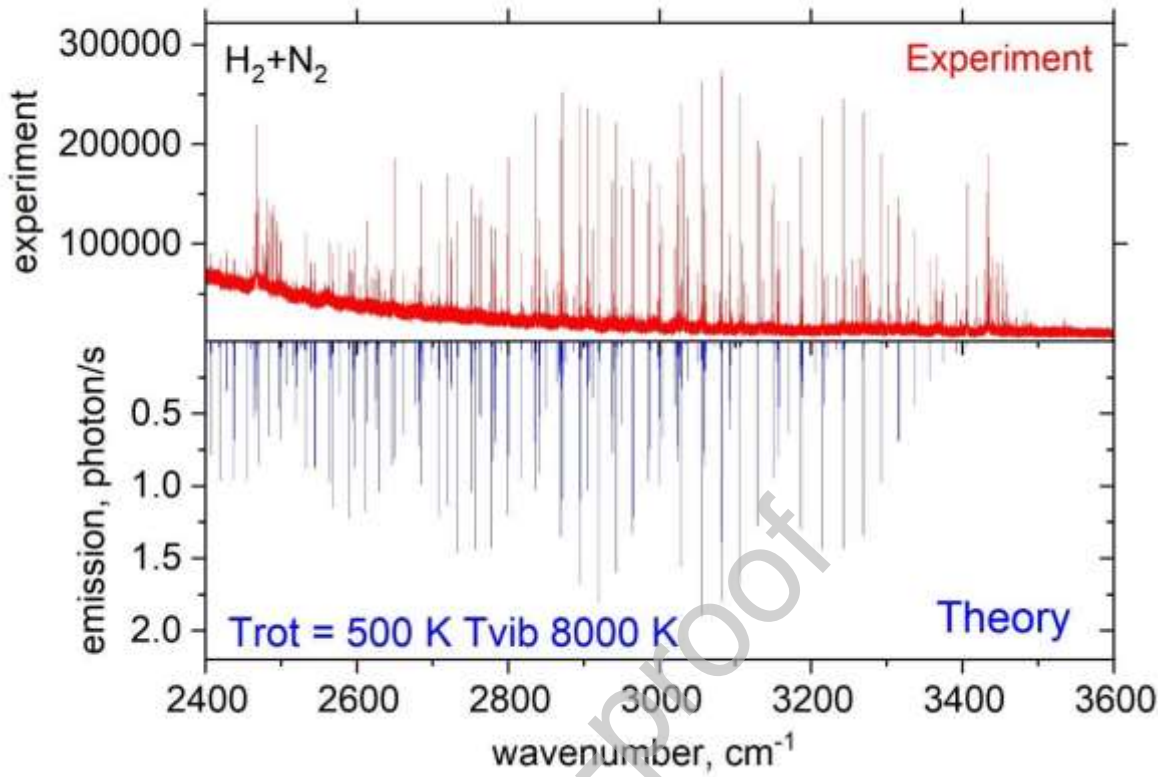

Figure 11: Experiment (red) versus bi-temperature (blue) modelling of the NH spectra between 2400-3600 cm^{-1} obtained from the H_2 + N_2 mixture. The theoretical spectrum corresponds to the non-LTE combination of T_R = 500 K, T_v = 8000 cm^{-1}, Lorentzian line profile and a HWHM = 0.02 cm^{-1}. The MoLLIST[42,43] line list was used

Conclusion

1.

In this work, a time resolved spectroscopic study of a pulsed positive column discharge of two mixtures, NH_3 + N_2 + Ar and H_2 + N_2 + He, in the spectral range of 1923-3571 cm^{-1} is presented, measured with a microsecond time scale and spectral resolution of 0.02 cm^{-1}. The detailed analysis of the time-dependent profiles of the individual lines was performed, provided the valuable information about the population of observed states and individual lifetimes. The lifetimes of the studied states were shown to decrease with increasing vibrational quantum number, which is in accordance with our previous discovery of the same trend in CN radical spectra.

2.

We used the accurate MoLLIST line list for NH to model the experimental spectra of NH for both mixture sNH_3 + N_2 + Ar and H_2 + N_2 + He, which provided additional information on the population of the excited vibrational states involved in the discharge and revealed their effective (rotational and vibrational) temperatures. The NH spectrum of produced in the NH_3 + N_2 + Ar glow discharge mixture was found to be in LTE with the average temperature of T = 6000 K, with the vibrational temperature estimated as T_V = 5999 ± 1125 K. The H_2 + N_2 + He spectrum however exhibits a clear non-LTE bi-temperature behaviour with T_R = 500 K, T_V = 8000 K.

3.

A rotational spectrum of the NH free radical (measured in the NH_3 + N_2 + Ar mixture) in the ground $X^3\Sigma^-$ electronic state has been observed using the time-resolved Fourier transform spectroscopy in the frequency region of 10-13 μm. 12 triplet-resolved high rotationally excited pure rotation lines of NH have been observed in the lab and compared with ATMOS and ACE solar data.

Acknowledgments

This work was funded by grant no CZ.02.1.01/0.0/0.0/16_019/0000778 alias "ERDF/ESF Centre of Advanced Applied Sciences". This work was also supported by UK research councils EPSRC, under grant EP/N509577/1, and STFC, under grant ST/R000476/1. This work made extensive use of the STFC DiRAC HPC facility supported by BIS National E-infrastructure capital grant ST/J005673/1 and STFC grants ST/H008586/1 and ST/K00333X/1. We thank the European Research Council (ERC) under the European Union's Horizon 2020 research and innovation programme through Advance Grant number 883830.

Author contribution statement (CRediT style)

Adam Pastorek – Formal analysis, Investigation, Visualization, Data curation, Writing – original draft, Writing – review & editing

Victoria H. J. Clark – Data curation, Writing – original draft

Sergei N. Yurchenko - Data curation, Writing – original draft, Supervision, Validation

Svatopluk Civiš – Conceptualization, Writing – review & editing, Funding acquisition, Supervision, Validation

Declaration of interests

☒ The authors declare that they have no known competing financial interests or personal relationships that could have appeared to influence the work reported in this paper.

☐ The authors declare the following financial interests/personal relationships which may be considered as potential competing interests:

References

1. Bernath, P. F. & Amano, T. Difference frequency laser spectroscopy of the v = 1 ← 0 transition of NH. *J. Mol. Spectrosc.* **95**, 359–364 (1982).

2. Boudjaadar, D., Brion, J., Chollet, P., Guelachvili, G. & Vervloet, M. Infrared emission spectra of five Δv = 1 sequence bands of the free radical NH in its X3Σ- state. *J. Mol. Spectrosc.* **119**, 352–366 (1986).

3. Brooke, J. S. A., Bernath, P. F., Western, C. M., van Hemert, M. C. & Groenenboom, G. C. Line strengths of rovibrational and rotational transitions within the X3Σ− ground state of NH. *J. Chem. Phys.* **141**, 054310 (2014).

4. Lewen, F., Brünken, S., Winnewisser, G., Šimečková, M. & Urban, Š. Doppler-limited rotational spectrum of the NH radical in the 2 THz region. *J. Mol. Spectrosc.* **226**, 113–122 (2004).

5. Stewart, K. The imine radical, NH. *Trans. Faraday Soc.* **41**, 663 (1945).

6. Van Helden, J. H. *et al.* Production mechanisms of NH and NH2 radicals in N 2-H2 plasmas. *J. Phys. Chem. A* **111**, 11460–11472 (2007).

7. Eder, J. M. Beiträge zur Spectralanalyse. *Denksch. Wien. Akad.* **60**, 1–12 (1893).

8. Fowler, A. & Gregory, C. C. L. The Ultra-Violet Band of Ammonia, and Its Occurrence in the Solar Spectrum. *Philos. Trans. R. Soc. London* **218**, 351–372 (1919).

9. Funke, G. W. Das Absorptionsspektrum des NH. *Zeitschrift für Phys.* **101**, 104–112 (1936).

10. Dixon, R. N. THE 0–0 AND 1–0 BANDS OF THE A (3 Π i)– X (3 Σ −) SYSTEM OF NH. *Can. J. Phys.* **37**, 1171–1186 (1959).

11. Ram, R. S., Bernath, P. F. & Hinkle, K. H. Infrared emission spectroscopy of NH: Comparison of a cryogenic echelle spectrograph with a Fourier transform spectrometer. *J. Chem. Phys.* **110**, 5557–5563 (1999).

12. Mantei, K. A. & Bair, E. J. Reactions of nitrogen-hydrogen radicals. III. Formation and disappearance of NH radicals in the photolysis of ammonia. *J. Chem. Phys.* **49**, 3248–3256 (1968).

13. Hansen, I., Hoinghaus, K., Zetzsch, C. & Stuhl, F. Detection of NH (X p3Σ−) by resonance fluorescence in the pulsed vacuum uv photolysis of NH3 and its application to reactions of NH radicals. *Chem. Phys. Lett.* **42**, 370–372 (1976).

14. Brazier, C. R., Ram, R. S. & Bernath, P. F. Fourier transform spectroscopy of the A3Π-X3Σ- transition of NH. *J. Mol. Spectrosc.* **120**, 381–402 (1986).

15. Clement, S. G., Ashfold, M. N. R., Western, C. M., Johnson, R. D. & Hudgens, J. W. Triplet excited states of the NH(ND) radical revealed via two photon resonant multiphoton ionization spectroscopy. *J. Chem. Phys.* **96**, 5538–5540 (1992).

16. Swings, P., Elvey, C. T. & Babcock, H. W. The Spectrum of Comet Cunningham,

1940C. *Astrophys. J.* **94**, 320 (1941).

17. Singh, P. D. & Gruenwald, R. B. The photodissociation lifetimes of the NH radical in comets. *Astron. Astrophys.* **178**, 277–282 (1987).

18. Sneden, C. The nitrogen abundance of the very metal-poor star HD 122563. *Astrophys. J.* **184**, 839 (1973).

19. Lambert, D. L., Brown, J. A., Hinkle, K. H. & Johnson, H. R. Carbon, nitrogen, and oxygen abundances in Betelgeuse. *Astrophys. J.* **284**, 223 (1984).

20. Smith, V. V. & Lambert, D. L. The chemical composition of red giants. II - Helium burning and the s-process in the MS and S stars. *Astrophys. J.* **311**, 843 (1986).

21. Aoki, W. & Tsuji, T. High resolution infrared spectroscopy of CN and NH lines: nitrogen abundance in oxygen-rich giants through K to late M. *Astron. Astrophys.* **328**, 175–186 (1997).

22. Meyer, D. M. & Roth, K. C. Discovery of interstellar NH. *Astrophys. J.* **376**, L49 (1991).

23. Crawford, I. A. & Williams, D. A. Detection of interstellar NH towards ζ Ophiuchi by means of ultra-high-resolution spectroscopy. *Mon. Not. R. Astron. Soc.* **291**, (1997).

24. Weselak, T., Galazutdinov, G. A., Beletsky, Y. & Krełowski, J. Interstellar NH molecule in translucent sightlines. *Mon. Not. R. Astron. Soc.* **400**, 392–397 (2009).

25. Spite, M. *et al.* First stars VI - Abundances of C, N, O, Li, and mixing in extremely metal-poor giants. Galactic evolution of the light elements. *Astron. Astrophys.* **430**, 655–668 (2005).

26. Claxton, T. A. Ab initio UHF calculations. Part 3.—NH radicals. *Trans. Faraday Soc.* **66**, 1540–1543 (1970).

27. Das, G., Wahl, A. C. & Stevens, W. J. Ab initio study of the NH radical. *J. Chem. Phys.* **61**, 433–434 (1974).

28. Ram, R. S. & Bernath, P. F. Revised molecular constants and term values for the X3Σ- and A3Π states of NH. *J. Mol. Spectrosc.* **260**, 115–119 (2010).

29. Brooke, J. S. A., Bernath, P. F. & Western, C. M. Note: Improved line strengths of rovibrational and rotational transitions within the X 3 Σ − ground state of NH . *J. Chem. Phys.* **143**, 026101 (2015).

30. Fernando, A. M., Bernath, P. F., Hodges, J. N. & Masseron, T. A new linelist for the A3Π–X3Σ− transition of the NH free radical. *J. Quant. Spectrosc. Radiat. Transf.* **217**, 29–34 (2018).

31. van de Meerakker, S. Y. T., Jongma, R. T., Bethlem, H. L. & Meijer, G. Accumulating NH radicals in a magnetic trap. *Phys. Rev. A - At. Mol. Opt. Phys.* **64**, 4 (2001).

32. Van De Meerakker, S. Y. T., Labazan, I., Hoekstra, S., Küpper, J. & Meijer, G. Production and deceleration of a pulsed beam of metastable NH (a 1Δ) radicals. *J. Phys. B At. Mol. Opt. Phys.* **39**, (2006).

33. Plomp, V., Gao, Z., Cremers, T. & Van De Meerakker, S. Y. T. Multistage Zeeman deceleration of NH X Σ - 3 radicals. *Phys. Rev. A* **99**, 1–6 (2019).

34. Pastorek, A., Civiš, S., Clark, V. H. J., Yurchenko, S. N. & Ferus, M. Time-resolved Fourier transform infrared emission spectroscopy of CO Δv = 1 and Δv = 2 extended bands in the ground X1Σ+ state produced by formamide glow discharge. *J. Quant. Spectrosc. Radiat. Transf.* **262**, 107521 (2021).

35. Horká, V., Civiš, S., Špirko, V. & Kawaguchi, K. The infrared spectrum of CN in its ground electronic state. *Collect. Czechoslov. Chem. Commun.* **69**, 73–89 (2004).

36. Ferus, M. *et al.* HNC/HCN ratio in acetonitrile, formamide, and BrCN discharge. *J. Phys. Chem. A* **115**, 1885–1899 (2011).

37. Ferus, M. *et al.* Prebiotic synthesis initiated in formaldehyde by laser plasma simulating high-velocity impacts. *Astron. Astrophys.* **626**, A52 (2019).

38. Civiš, S., Šedivcová-Uhlíková, T., Kubelík, P. & Kawaguchi, K. Time-resolved Fourier transform emission spectroscopy of A2Π-X2Σ+ infrared transition of the CN radical. *J. Mol. Spectrosc.* **250**, 20–26 (2008).

39. Farmer, C. B. & Norton, R. H. A high-resolution atlas of the infrared spectrum of the sun and the earth atmosphere from space. A compilation of ATMOS spectra of the region from 650 to 4800 cm-1 (2.3 to 16 microns). *NASA Ref. Publ. 1224* **2**, (1989).

40. Geller, M., Sauval, A. J., Grevesse, N., Farmer, C. B. & Norton, R. H. First identification of pure rotation lines of NH in the infrared solar spectrum. *Astron. Astrophys.* **249**, 550–552 (1991).

41. Hase, F., Wallace, L., McLeod, S. D., Harrison, J. J. & Bernath, P. F. The ACE-FTS atlas of the infrared solar spectrum. *J. Quant. Spectrosc. Radiat. Transf.* **111**, 521–528 (2010).

42. Bernath, P. F. MoLLIST: Molecular Line Lists, Intensities and Spectra. *J. Quant. Spectrosc. Radiat. Transf.* **240**, (2020).

43. Wang, Y., Tennyson, J. & Yurchenko, S. N. Empirical line lists in the ExoMol database. *Atoms* **8**, (2020).

44. Yurchenko, S. N., Al-Refaie, A. F. & Tennyson, J. EXOCROSS: a general program for generating spectra from molecular line lists. *Astron. Astrophys.* **614**, A131 (2018).

45. Treanor, C. E., Rich, J. W. & Rehm, R. G. Vibrational relaxation of anharmonic oscillators with exchange-dominated collisions. *J. Chem. Phys.* **48**, 1807–1813 (1968).

46. Pannier, E. & Laux, C. O. RADIS: A nonequilibrium line-by-line radiative code for CO2 and HITRAN-like database species. *J. Quant. Spectrosc. Radiat. Transf.* **222**–**223**, 12–25 (2019).